Reorientations in the Bacteriorhodopsin Photocycle†

Qin Song, Greg S. Harms, Chaozhi Wan, and Carey K. Johnson*

Department of Chemistry, University of Kansas, Lawrence, Kansas 66045

Received February 9, 1994; Revised Manuscript Received September 6, 1994®

ABSTRACT: Reversible photoinduced reorientations of bacteriorhodopsin have been detected in suspensions of the purple membrane of *Halobacterium salinarium.* The anisotropy in bacteriorhodopsin during the nanosecond through millisecond stages of the photocycle was measured by time-resolved linear dichroism and transient absorption measurements. From these measurements the anisotropies of the K, L, M, and O intermediates were determined and related to the chromophore orientation with respect to the initially selected orientation. The anisotropies of the K and L states are 0.38 ± 0.01 and 0.35 ± 0.01, respectively. Further anisotropy decay after formation of the M intermediate in about 0.5 ms is evidence of orientational motion at this stage in the photocycle. A constant anisotropy with a value of 0.39 ± 0.02 in the O intermediate demonstrates a recovery of the initial protein orientation with the formation of the O state. These results demonstrate that reorientations in BR are photoinduced and reversible. Similar measurements for L and M were carried out for purple membrane in polyacrylamide gels, where the anisotropies in the L and M states are 0.38 ± 0.014 and 0.36 ± 0.01, respectively. These results show that reorientations also occur in BR immobilized in gels. Anisotropy decay in the M state after formation of the M intermediate was not detected in the gels, in contrast to the M intermediate in suspensions. Orientational changes are observed for BR in purple membrane suspensions in the K state, during the K → L step, in the M state possibly related to an $M_1 \rightarrow M_2$ transition, and in the O state, where an almost complete return to the original orientation occurs. For BR in gels, reorientations are reduced but not abolished. The possible role of these reorientations in bacteriorhodopsin is discussed.

Proton pumping by membrane proteins plays an essential role in energy transduction in biological systems. A fascinating example is bacteriorhodopsin (BR),[1] a photoactive membrane protein which transduces light energy into chemical potential by pumping protons across the cell membrane. BR (molecular weight 26 K) is embedded in the purple membrane of *Halobacterium salinarium* and organized in trimeric unit cells arranged in a two-dimensional hexagonal lattice. A retinal Schiff base, covalently linked to each protein, is responsible for light absorption, which triggers *trans* to *cis* isomerization followed by a sequence of ground-state transient intermediates, J → K → L → M → N → O → BR [for recent reviews, see Mathies et al. (1991) and Birge (1990)]. In the L → M step, the retinal Schiff base deprotonates. Since Asp-85 is protonated simultaneously (Braiman et al., 1988; Gerwert et al., 1990), it apparently serves as the corresponding proton acceptor. The Schiff base is reprotonated in the M → N step (Fodor et al., 1988). Asp-96 has been implicated (Gerwert et al., 1989; Otto et al., 1989; Braiman et al., 1991) as a possible proton donor. The *all-trans* conformation of the retinal Schiff base is restored with the formation of the O intermediate (Smith et al., 1983), while a proton is taken from the cytoplasmic side of the membrane and Asp-96 is reprotonated (Holz et al., 1989; Otto et al., 1989).

Time-resolved experiments sensitive to protein motions are needed to elucidate the role of protein motions in bacteriorhodopsin. The recent structural model of BR determined by electron diffraction methods (Henderson et al., 1990) establishes the basis for understanding the mechanism of proton pumping in BR. Based on both structural and spectroscopic data, models of the proton-pumping mechanism have been proposed (Fodor et al., 1988; Braiman et al., 1988; Henderson et al., 1990; Mathies et al., 1991) in which protein conformational changes play a vital functional role in the proton transport mechanism. Mathies and co-workers proposed a "C-T" model, wherein *trans* to *cis* isomerization triggers a transition from the T-form of the protein (the preferred conformation for the *all-trans* chromophore) to the C-form, which accommodates the 13−*cis* chromophore (Fodor et al., 1988; Mathies *et al.*, 1991). Henderson and collaborators (1990), on the other hand, envisioned three protein conformations, associated with the BR → K, L → M, and M → N portions of the photocycle. A protein conformational change in the M state could serve as a "reprotonation switch" to prevent back transfer of the proton released by the Schiff base (Fodor et al., 1988).

Orientational motion in BR has been investigated previously by linear dichroism spectroscopy, which detects reorientation of the retinal chromophore following polarization-selective excitation of BR (Lozier & Niederberger, 1977; Sherman & Caplan, 1977; Cherry et al., 1977; Godfrey, 1982; Czégé et al., 1982; Ahl & Cone, 1984; Der et al., 1988; Otto & Heyn, 1991). Based on a thorough study of the dichroism at several wavelengths, Ahl and Cone (1984) attributed anisotropy changes detected with ~1-ms resolution to the rotation of monomeric proteins within the trimer in the BR membrane. Results from diffraction studies (Koch et al., 1991; Dencher et al., 1989; Subramaniam et al., 1993), on the other hand, point to tertiary structural changes within BR monomers.

† This work was supported by Grant GM 40071 from the National Institutes of Health.

® Abstract published in *Advance ACS Abstracts,* October 15, 1994.

[1] Abbreviations: BR, bacteriorhodopsin; TRLD, time-resolved linear dichroism; TA, transient absorption.

0006-2960/94/0433-14026$04.50/0

Recent work in our laboratory (Wan et al., 1993) has demonstrated that activation of one BR induces reorientations in neighboring "spectator" proteins in the trimer within the purple membrane. The present work extends these studies to span the photocycle of BR, and to map out the anisotropies at each stage of the photocycle. This work together with our previous report (Wan et al., 1991) represents the first direct observation of protein reorientational motions with time resolution sufficient to resolve these motions throughout the BR photocycle. Evidence is presented for reorientation *before* the formation of the M intermediate, and for a reorientation of the M intermediate itself in less that 1 ms. We find that the initial orientation is subsequently almost fully recovered in the O intermediate on the millisecond time scale. Orientational motions are discussed in the context of the recently published structure (Henderson et al., 1990) and models of the proton-pumping mechanisms, and a possible link to reorientations of neighboring spectator proteins (Wan et al., 1993).

EXPERIMENTAL PROCEDURES

The experimental arrangement is identical to that used in previous TRLD experiments (Wan et al., 1991, 1993). The pump beam was polarized vertically, and the probe beam was oriented at 45° with respect to the pump polarization. The analyzing polarizer was oriented to select the vertical and horizontal components of the probe beam. Special care was taken to assure precise alignment of the two probe-beam polarizers. The polarizer P_{pr} preceding the sample was set at 45° from vertical, and the analyzing polarizer P_{an} following the sample was oriented at 0°. These polarizers were mounted in high resolution rotation stages (6 arc·s resolution) and set as follows. P_{an} was first adjusted to be parallel (±0.05°) to the pump polarization by rotating it to achieve minimum intensity of the rejected pump beam. This defines 0° for P_{an}. Then, P_{an} was rotated by precisely 45°, and P_{pr} was adjusted to extinguish the transmitted probe beam. This sets P_{pr} to transmit light polarized at 45° with respect to the pump polarization. Finally, P_{an} was returned to 0° to separate the vertically and horizontally polarized components of the probe beam. The resulting experimental setup is shown in Figure 2 of Wan et al. (1991).

The excitation pulse energy at 532 nm in these experiments was less than 0.1 μJ with a 0.1−0.2 mm beam diameter. The energy of the probe pulses was limited to less than 0.01 μJ with neutral optical density filters. The laser system (Johnson et al., 1988) generates pump and probe pulses of about 50 ps duration with time delays between pump and probe variable from the picosecond to the second time scales. The pulse repetition rate of 30 Hz was selected so that the time between two sequential pump pulses was longer than the photocycle completion time. The probe signals with polarizations parallel and perpendicular to the excitation pulse, $I_{\parallel}$ and $I_{\perp}$, selected by the analyzing polarizer were detected by large-area photodiodes. The probe pulse intensity was also sampled by another photodiode to generate a reference signal (I_o). This intensity was set equal to $I_{\parallel}$ and $I_{\perp}$ with the pump beam blocked by means of a variable neutral density filter. Parallel, perpendicular, and reference signals were processed by gated integrators. Both the parallel and perpendicular signals were divided by the reference signal to compensate for pulse-to-pulse fluctuations, and the resulting ratios were digitized and stored in a computer for analysis. In order to correct for any base-line drift, a shutter was used to block and unblock the pump pulse at about 1-s intervals, and the difference signal was recorded. This significantly enhanced the accuracy and reproducibility of anisotropy measurements. For weak signals (e.g., measurements at 690 nm), the pump beam was also chopped at half the laser repetition rate, and the signals $I_0 - I_{\parallel}$ and $I_0 - I_{\perp}$ from the output of the gated integrators were amplified by lock-in amplifiers.

The time-dependent absorption signals parallel [$\Delta A_{\parallel} = \log(I_0/I_{\parallel})$] and perpendicular [$\Delta A_{\perp} = \log(I_0/I_{\perp})$] to the pump polarization were measured at several probe wavelengths from 410 to 690 nm. The TRLD, $D(t) = \Delta A_{\parallel} - \Delta A_{\perp}$, the isotropic transient absorption (TA), $\Delta A = \Delta A_{\parallel} + 2\Delta A_{\perp}$, and the anisotropy, $r = (\Delta A_{\parallel} - \Delta A_{\perp})/(\Delta A_{\parallel} + 2\Delta A_{\perp})$, were calculated from the digitized signals. This method allows us to measure the parallel and perpendicular absorption simultaneously and thus precisely to compare the transient absorption and linear dichroism.

The purple membrane was extracted from *H. salinarium* strain ET1−001 by standard methods (Oesterhelt & Stoeckenius, 1974) and suspended in phosphate buffer (10 mM with 5 mM azide) at pH 7. The sample was light adapted by exposure to a 100-W lamp. Light adaptation was verified by the shift in the absorption maximum from 558 nm in dark-adapted BR to 568 nm in light-adapted BR. The sample was flowed at 25 °C through a 2-mm-thick sample cell at a rate of 1−4 mm s^{-1} in order to prevent repetitive excitation and sample heating. There is no detectable flow orientation at this flow rate. With no pump pulses, the dichroism remained zero as the flow rate was varied from 0 to 10 mm s^{-1}. The gel samples were prepared by combining purple membrane suspended in pH 7.0 phosphate buffer with 3% or 7.5% (w/v) acrylamide, 0.1% or 0.2% (w/v) bis(acrylamide), and 0.03% (w/v) tetramethylethylenediamine. The solution was degassed by vacuum for 15 min. Then, 0.2% (w/v) ammonium persulfate was added to catalyze the polymerization. The liquid was immediately poured into a 5.0 mm path length sample cell, sealed, and allowed to polymerize for 30−60 min. The sample cell was rotated during data collection to prevent repetitive excitation and sample heating. Liquid and gel samples were optically clear with an optical density in the sample cell of about 1−1.6 at 568 nm. The sample temperature for all measurements was 25 °C.

RESULTS

Anisotropy measurements of two types have been made. Figures 1−3 show time-dependent anisotropy scans. In addition, we measured the anisotropy at fixed times at several wavelengths. These measurements were signal averaged in order to achieve precise measurements of the anisotropy, and the pump power was reduced until the measured anisotropy was independent of pump power. These precautions, together with careful control of signal offsets and base-line drifts (see Experimental Procedures), allow accurate anisotropy measurements. The results of these fixed-time anisotropy measurements are tabulated in Table 1.

The experimentally determined anisotropies are both wavelength and time dependent. Since the measured anisotropy at a given time may contain contributions from any

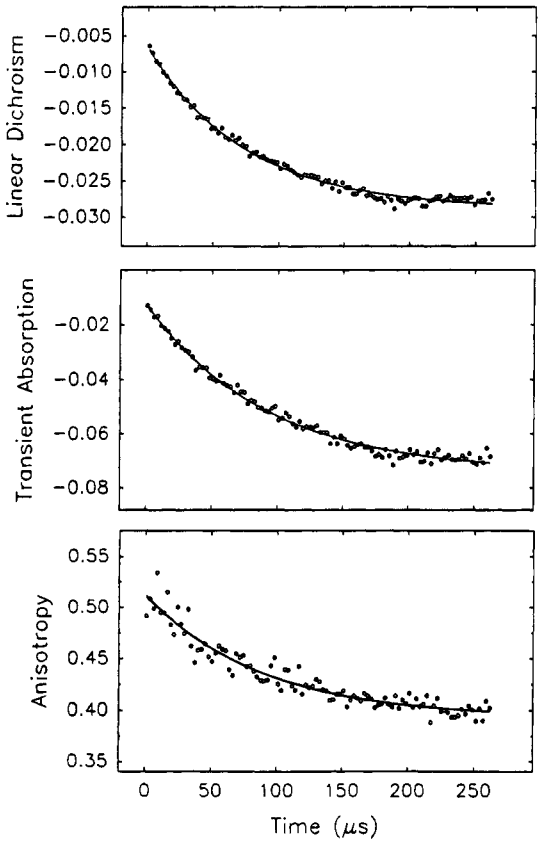

FIGURE 1: Anisotropy (bottom panel), transient absorption (middle panel), and time-resolved linear dichroism (top panel) of bacteriorhodopsin at a probe wavelength of 560 nm on the submillisecond time scale. All three quantities were calculated from absorbance changes $\Delta A_{\parallel}$ and $\Delta A_{\perp}$ as described in the text. The solid lines show single-exponential fits to the decays with time constants of 88 ± 8 μs for the anisotropy decay, 93 ± 3 μs for the transient absorption, and 74.7 ± 2 μs for the linear dichroism. (Uncertainties are the standard errors in the least-squares fits.)

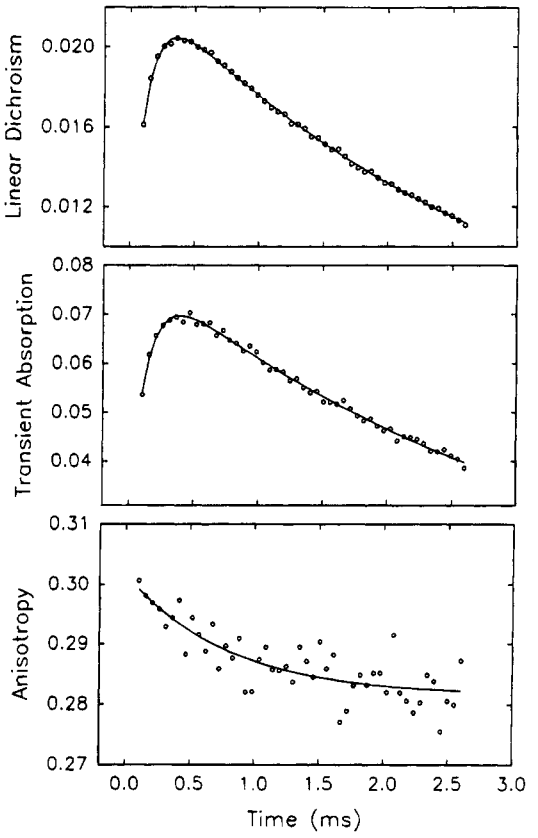

FIGURE 2: Anisotropy (bottom panel), transient absorption (middle panel), and time-resolved linear dichroism (top panel) of bacteriorhodopsin at a probe wavelength of 410 nm over 3 ms. The solid line shows a single-exponential fit to the anisotropy decay with a time constant of 786 ± 240 μs. The TA and TRLD are fit to double-exponential functions. (TA: rise time 120 ± 11 μs, decay time 3.39 ± 0.61 ms; TRLD: rise time 119 ± 4 μs, decay time 2.96 ± 0.18 ms. Uncertainties are the standard errors from the least-squares fits.) The pump-pulse energy required for this scan resulted in a reduction of anisotropy values due to saturation (see Figure 4). Nonsaturated M-state anisotropies recorded at a fixed time delay of 390 μs are shown in Table 1.

photocycle intermediates present at that time as well as from the ground state, the anisotropy of a given photocycle intermediate cannot be determined directly. The anisotropy $r_\lambda(t)$ measured in these experiments contains contributions from each species whose absorption profile overlaps the probe wavelength:

$$r_\lambda(t) = \sum_i r_i(t) \frac{\Delta A_i(\lambda,t)}{\Delta A(\lambda,t)} \quad (1)$$

where $r_i(t)$ is the anisotropy of species i, $\Delta A_i(\lambda,t)$ is the TA of species i, and $\Delta A(\lambda,t)$ is the total TA given by $\Delta A_{\parallel}(\lambda,t) + 2\Delta A_{\perp}(\lambda,t)$. At 410 and 690 nm, the experimental anisotropy is dominated by a single species, intermediate M or O, respectively. At 550−570 nm, on the other hand, both the BR ground state and the L or N intermediates can contribute (Wan et al., 1993).

The anisotropy measured at 560 nm is shown in Figure 1 for time delays on the microsecond time scale. The anisotropy at 560 nm decays from ≥0.50 to 0.40. The initial anisotropy is clearly larger than the maximum anisotropy of 0.40 expected for a single transition. The solid lines through the data show single-exponential fits to the decays. The time constants (see caption to Figure 1) are consistent with the L → M decay time determined from the transient absorption scan.

Anisotropy in the L and BR States. At early times, both the BR hole (ground-state depletion) and the L state contribute to this signal, and the measured TA is $\Delta A = \Delta A_{BR} + \Delta A_L$ (where the time and wavelength dependence are suppressed for simplicity). The measured anisotropy at 560 nm is then given by

$$r_\lambda = r_{BR} + \frac{\Delta A_L}{\Delta A}(r_L - r_{BR}) \quad (2)$$

After 250 μs, $\Delta A_L \approx 0$, and the anisotropy of the ground-state hole, r_{BR}, is measured directly. The decay in Figure 1 shows $r_{BR} \approx 0.4$ at this point. This value of the anisotropy r_{BR} is important for two reasons. First, the measurement of the maximum theoretically possible value of the anisotropy of BR shows that the anisotropy is not reduced due to saturation with the pump intensity employed. Second, this measurement shows that no anisotropy decay occurs in the BR ground-state hole prior to this time delay. We conclude that $r_{BR} = 0.4$ over the time delays spanned by Figure 1. Since the overall transient absorption ΔA is negative at 560 nm, ΔA and ΔA_L (the contribution of the L state to the total absorbance change) have opposite sign. Hence, these results show that $r_L < r_{BR}$.

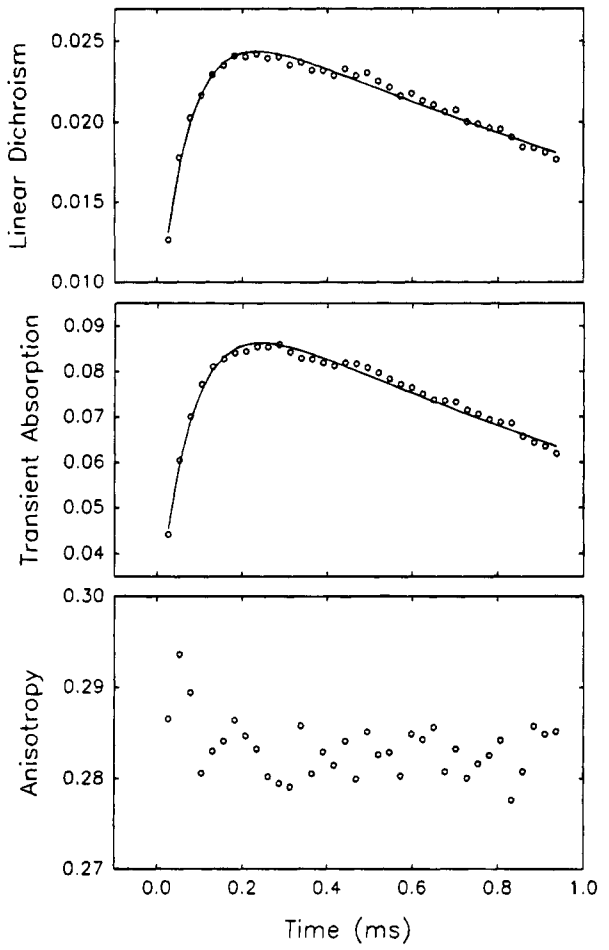

FIGURE 3: Anisotropy (bottom panel), transient absorption (middle panel), and time-resolved linear dichroism (top panel) of bacteriorhodopsin in a 3% gel at a probe wavelength of 410 nm. The solid lines show double-exponential fits to the TA and TRLD decays. (TA: rise time 78 ± 5 μs; decay time 2.41 ± 0.68 ms; TRLD: rise time 72 ± 4 μs; decay time 3.26 ± 1.13 ms.) The pump-pulse energy required for this scan resulted in a reduction of anisotropy values due to saturation (see Figure 4). Nonsaturated M-state anisotropies recorded at a fixed time delay of 390 μs are shown in Table 1. The nonsaturated measurements in Table 1 demonstrate that less reorientation occurs in gels than in suspension. A comparison of Figures 2 and 3 shows that reorientation in the M state as observed in suspension is absent or limited (to $\Delta r < 0.01$) in gels.

The anisotropy of L can be determined from the measured anisotropy r_λ, the anisotropy of BR, r_{BR}, and the ratio ($\Delta A_L/\Delta A$). This ratio can be obtained from the absorbance changes in Figure 1. Precise values of r_λ and ΔA at 560 nm were obtained by signal averaging at fixed delay times of 10 and 390 μs. These results are listed in Table 1. At 390 μs, after $\Delta A_L(t)$ has decayed to zero, $\Delta A = \Delta A_{BR}$. From the values of ΔA, ΔA_{BR}, and r_λ at 10 and 390 μs, the anisotropy of the L state is determined to be $r_L = 0.35 \pm 0.01$ in suspension and $r_L = 0.381 \pm 0.014$ in a 7.5% gel.

On a longer time scale, the anisotropy at 560 nm decays to zero in about 15 ms (data not shown). This result is consistent with previous measurements on this time scale at several wavelengths in the 550−590 nm region (Wan et. al, 1993). The anisotropy behavior at these wavelengths in the millisecond time regime was discussed previously and was associated with reorientational motion of "spectator" proteins neighboring the excited BR in the trimer (Wan et al., 1993).

Table 1: Anisotropies $r_\lambda(t)$ in the Bacteriorhodopsin Photocycle Measured with Nonsaturating Pump-Pulse Energies

probe wavelength (nm)	sample	time delay	state	$r_\lambda(t)$[a]	θ[b] (deg)
640	suspension	10 ns	K	0.380 ± 0.010	11
560	suspension	10 μs	BR, L	0.560 ± 0.008	
560	suspension	10 μs	L[c]	0.35 ± 0.01	17
560	suspension	390 μs	BR	0.395 ± 0.007	
410	suspension	390 μs	M	0.33 ± 0.02	20
690	suspension	4.0 ms	O	0.389 ± 0.015	8
560	3% gel	6−13 μs	L[c]	0.377 ± 0.013	11
560	7.5% gel	6−13 μs	L[c]	0.381 ± 0.014	10
560	3% gel	260−390 μs	BR	0.411 ± 0.012	
560	7.5% gel	390 μs	BR	0.406 ± 0.022	
410	3% gel	390 μs	M	0.36 ± 0.02	15
410	7.5% gel	390 μs	M	0.36 ± 0.01	15

[a] Reported uncertainties are the standard error. [b] Reorientation with respect to orientation at $t = 0$ calculated from eq 5, with all proteins assumed to undergo the same reorientation. [c] Calculated from eq 2.

M-State Anisotropy. Figure 2 shows the anisotropy of M at 410 nm recorded on a time scale of 0−2 ms. An anisotropy change $\Delta r \approx 0.02$ is observed. We have observed an anisotropy decay of this magnitude reproducibly on the submillisecond time scale. The solid line in Figure 2 shows a fit to a model for restricted orientational motion (Wan et al., 1991):

$$r(t) = r(\infty) + \Delta r \exp(-t/\tau_r) \quad (3)$$

where $r(\infty)$ is the limiting anisotropy, $\Delta r = r(0) - r(\infty)$ is the anisotropy change, and τ_r is the anisotropy decay time. This model fits the data well between 400 μs and 3 ms. For the fit in Figure 2, $\Delta r = 0.02 \pm 0.006$ and $r(\infty) = 0.282 \pm 0.002$. An average of two such measurements yields $\tau_r = 0.53 \pm 0.21$ ms. While some uncertainty exists in the absolute values of the measured anisotropy in repeated measurements, the anisotropy *change* is measured with much greater precision.

The experimental anisotropy at 410 nm is related to the anisotropies of M and BR by

$$r_{410} = r_M + (r_{BR} - r_M)\frac{\Delta A_{BR}(410\text{ nm})}{\Delta A(410\text{ nm})} \quad (4)$$

Over the time range of Figure 2, the contribution at 410 nm from the second term in eq 4 is small ($\leq$0.02) and nearly constant on this time scale. We cannot account for the time dependence in Figure 2 with a constant r_M and realistic values and time dependencies of the other parameters in eq 4. Hence, the anisotropy change measured at 410 nm is dominated by the anisotropy of the M intermediate, and the anisotropy decay reflects the time dependence of r_M. The anisotropy at 410 nm on a longer time scale was found to be constant over a period of several milliseconds (data not shown), in agreement with previous measurements on this time scale (Wan et al., 1993).

The anisotropy at 410 nm for purple membrane in polyacrylamide gel was also measured. The results of fixed-time measurements for 3% and 7.5% gels are included in Table 1. Figure 3 shows a time-dependent scan over the 0−1 ms range. In contrast to the measurement for a purple membrane suspension in Figure 2, the anisotropy is constant after ~0.1 ms within the precision of the measurement

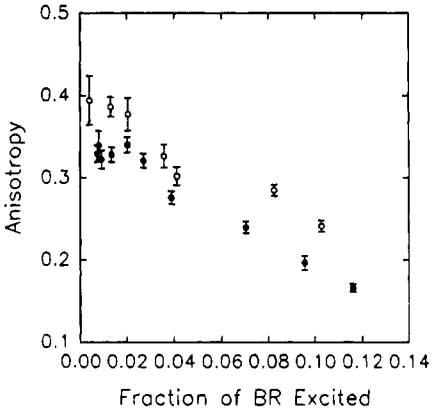

FIGURE 4: The dependence of the anisotropy at 410 nm (solid circles) and at 690 nm (open circles) on saturation by the pump pulse. The measured anisotropy is plotted as a function of the fraction of BR excited by the pump pulse. These measurements were recorded at time delays of 390 μs at 410 nm and 4.0 ms at 690 nm.

(<0.01). The scan may be suggestive of a possible anisotropy decay in <0.1 ms. However, the anisotropy signal at these time delays is noisy due to the low TA signal.

Another factor influencing the absolute value of the anisotropy is the excitation pulse energy. For the measurements at fixed time delays tabulated in Table 1, sufficiently weak pump pulses were used so that the measured anisotropy values are not reduced due to saturation by the pump pulse. The absence of saturation was verified by reducing the pump-pulse intensity with neutral density filters until anisotropies independent of pump power were measured. The dependence of the anisotropies measured at 410 and 690 nm on the extent of excitation is shown in Figure 4. For the data displayed in Figure 4, the fraction of BR excited at a given pump-pulse energy was calculated from the measured absorbance change ΔA, with the extinction coefficients and fractional concentrations of the M (at 410 nm) and O (at 690 nm) intermediates reported by Váró and Lanyi (1991). For both intermediates, we find that unsaturated anisotropy values are obtained when 2% or less of BR is excited. At 690 nm, for example, 2% excitation corresponds to an absorbance change ΔA of 0.003.

Although accurate measurements were possible under these conditions for signals averaged at fixed delay times, these signals were in some cases too weak for time-dependent scans. Hence, slightly saturating conditions were used for scans at 410 nm. This is the reason that the absolute value of the anisotropy in Figures 2 and 3 is lower than the value of r_M reported in Table 1. However, it has been shown that saturation by a short, intense light pulse affects only the absolute value of the anisotropy and does not affect its time dependence (Ansari & Szabo, 1993). Hence, the time constant for anisotropy decay (as in Figure 2) can be reliably determined under slightly saturated conditions, resulting in improved accuracy in the decay time due to reduced noise levels.

The absolute values of the anisotropy at 410 nm, $r_{410} = 0.33 \pm 0.02$ in suspensions and $r_{410} = 0.36 \pm 0.01$ in polyacrylamide gel, shown in Table 1, were measured with nonsaturating pump energies at a time delay of 390 μs, where the TA signal at 410 nm is at its peak. Based on these observations, it appears that less reorientation occurs in gels than in suspension. Since higher pump-pulse energies were required for the time-dependent scans in Figures 2 and 3, the anisotropy levels observed in these scans are lower due to saturation and do not accurately measure the absolute values of the M-state anisotropies. However, they do reflect anisotropy changes over this time range. The dependence of the measured anisotropies at 410 nm on pump intensity is shown in Figure 4. Although the time scans in Figures 2 and 3 were generated with higher, slightly saturating, pump intensities, the anisotropy decay in Figure 2 can be used to estimate the nonsaturated M-state anisotropy in the early (at ~100 μs) and late (after 1 ms) M intermediates, at time delays where the signals are too weak for nonsaturated anisotropy measurements. Since the anisotropy decays by about 0.01 in 400 μs, and $\Delta r = 0.02$ overall, the anisotropy at 410 nm at 100 μs is estimated to be 0.34, and the anisotropy after 1 ms is estimated to be 0.32. We stress again that the value of the anisotropy decrease, $\Delta r = 0.02$, has been determined with a significantly higher precision ($\pm$0.006) than the uncertainties reported in the absolute values of the anisotropy.

In order to determine the M-state anisotropy r_M, the measured anisotropy r_{410} must also be corrected for the contribution of ground-state BR at 410 nm. This correction can be estimated from eq 4. From available spectroscopic data (Váró & Lanyi, 1991), the ratio ΔA_{BR}(410 nm)/ΔA(410 nm) is approximately -0.41 at 100 μs (early M) and -0.34 at 1 ms (late M). The anisotropy r_{BR} is also needed for the correction in eq 4. The contribution of BR at 410 nm, ΔA_{BR}-(410 nm), may contain contributions from the $^1A_g^-$ state, whose transition dipole moment lies parallel to the stronger $^1B_u^+$ transition at 570 nm, and from the $^1A_g^+$ state, whose transition dipole moment lies perpendicular to the $^1B_u^+$ transition dipole (Birge, 1990). Contributions from these states could lead to a dependence of r_{BR} on wavelength. In particular, a contribution from the $^1A_g^+$ state at 410 nm could alter the anisotropy r_{BR} at 410 nm from the value of 0.4 measured at 560 nm after excitation at 532 nm. A value of 0.2 for the anisotropy probed at 560 nm following excitation at 337 nm has been reported (Dér et al., 1988). Although the value of r_{BR} at 410 nm is not known, it can reasonably be supposed to be equal to or less than 0.4 (its value if there is no contribution from a transition dipole perpendicular to the $^1B_u^+$ transition moment), but above 0.2, since the relative contribution of $^1A_g^+$ is expected to be weaker at 410 nm than 337 nm [Birge (1990) and references therein]. If $r_{BR} = 0.4$ at 410 nm, the anisotropy r_M calculated from eq 4 is 0.36 at 100 μs and 0.34 at 1 ms. At the lower limit, if $r_{BR} = 0.2$ at 410 nm, r_M is 0.30 for early M, and 0.29 for late M. In gels, the correction yields 0.37 if $r_{BR} = 0.4$, and 0.32 if $r_{BR} = 0.2$. Thus, while this correction adjusts the absolute value of the anisotropy r_M, it cannot account for the observed anisotropy change unless r_{BR} at 410 nm is assigned an unreasonably low value (<0.2). In this case, eq 4 shows that r_M would also be low (<0.3), indicating a larger anisotropy drop in the L $\rightarrow$ M transition.

O-State Anisotropy. The O-state anisotropy, r_o, was measured at 690 nm, on the red side of the O-state absorption band, in order to exclude contributions from any other species (including the BR ground state). Since the absorbance changes at 690 nm are weak, particular care was taken to avoid saturation of the anisotropy. The pump power dependence of the anisotropy at 690 nm at a time delay of

4 ms is plotted in Figure 4. The low-power limit gives the anisotropy of the O state, $r_o = 0.39$.

Comparison with Previous Measurements. While the measured anisotropies for the K and L states are consistent with the previous observation of an anisotropy drop associated with the K → L transition, the present more accurate measurements indicate that the K → L anisotropy decay is not as large as previously reported in our laboratory (Wan et al., 1991). We now think that an additional anisotropy decay due to rotational diffusion of small membrane particles present in those samples contributed to the previous measurements of lower anisotropies. In the work reported here, we have been unable to reproduce the observation of a ~2 μs rotational component and wavelength-dependent TRLD decay times. For the present experiments, sodium azide was added to the purple membrane preparations as a protease inhibitor. This appears to result in more stable sample preparations. The absence of significant contributions from rotational diffusion in the present results is verified by the high anisotropy (0.39) in the O state at a time delay of 4 ms.

Anisotropy changes in BR have been observed in several previous studies. [Ahl and Cone (1984) summarize reports appearing prior to their study]. Several studies have purported to show that anisotropy changes in BR are restricted when membrane fragments are immobilized in a gel. However, the anisotropies reported are not entirely mutually consistent. Czégé et al. (1982) report constant anisotropies of 0.35−0.38 at 410 nm and 0.30−0.35 at 550 nm for purple membrane in an agar gel (18 °C, pH 6.5) over 15 ms, while a constant anisotropy of ~0.38−0.40 at 410 nm was measured by Der et al. (1988) in a polyacrylamide gel at pH 5.5 (22 °C). More recently, reorientations of 2−3° were detected in the M state for BR in crystals at pH 5.6 (Schertler et al., 1991) and for oriented BR in a polyacrylamide gel at pH 7 (Otto & Heyn, 1991). In contrast, we have consistently found anisotropies at 560 nm >0.4 at 6−13 μs and ≃0.4 at 390 μs in 3% and 7.5% polyacrylamide gels, from which the anisotropies of L and BR could be determined with eq 2. The discrepancy between our determination of the anisotropy at 410 nm and the higher value reported by Der et al. (1988) is attributable to the effect of pH (G. S. Harms, Q. Song, and C. K. Johnson, unpublished results).

DISCUSSION

Anisotropies of Photocycle Intermediates. The TRLD and anisotropy measurements reported here probe directly the orientation of the retinylidene chromophore. The results demonstrate that the chromophore reorients with respect to the initially excited transition dipole over the course of the BR photocycle. The maximum reorientation is detected in the M state, after which the initial orientation is recovered (or nearly so) in the O state.

The anisotropy $r_i(t)$ of intermediate i is given by (Gordon, 1966)

$$r_i = \langle(3 \cos^2 \theta_i - 1)\rangle/5 \quad (5)$$

where θ_i is the angle between the initially excited transition dipole of BR and the transition dipole of intermediate i in the $t = 0$ molecular coordinate frame, and $\langle ... \rangle$ represents the orientational average over θ_i. Hence, θ_i is the angle by

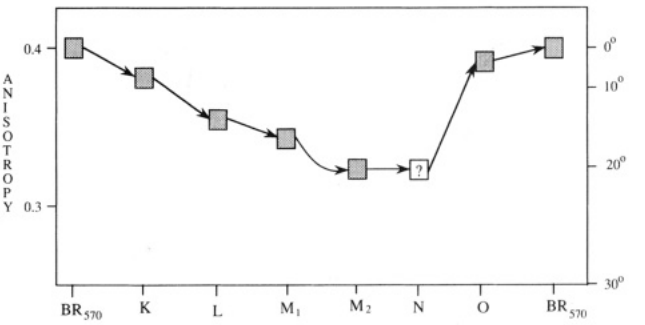

FIGURE 5: Summary of anisotropy changes in bacteriorhodopsin. The right-hand scale gives the reorientation angle obtained from eq 5 if all excited chromophores reorient by the same angle. M_1 and M_2 denote the early and late forms of the M intermediate. The anisotropy of N is not known and is assumed in this plot to be equal to the anisotropy of M. The anisotropy of M in this plot has not been corrected for the contribution of BR at 410 nm, since the anisotropy of BR at 410 nm is not known. This correction could shift the absolute value of the anisotropy of M_1 and M_2, but cannot account for the anisotropy decay between M_1 and M_2 (see text).

which the transition dipole of intermediate i at the time of the probe pulse has reoriented with respect to the BR transition dipole excited by the pump pulse. In general, the distribution function of θ_i is required in order to relate r_i to an average angle of reorientation. If all transition dipoles reorient by the same angle θ_i, a determination of the anisotropy of an intermediate yields the reorientation angle via eq 5. One should note that the anisotropy and linear dichroism are insensitive to changes in the azimuthal angle, that is, to rotational motion on a cone about the axis of the initially excited dipole. It is also not possible to distinguish between reorientations in the plane of the membrane and out of the plane by this experimental technique.

The anisotropies determined for the intermediates of the BR photocycle are summarized in Figure 5. Several studies have found that the kinetic sequence BR → K → L ↔ M ↔ N ↔ O → BR (with some variations) successfully accounts for the observed kinetic data in BR (Ames & Mathies, 1990; Nagle, 1991; Váró & Lanyi, 1991). This scheme is adopted in Figure 5 for purposes of discussion, although other kinetic models could also be considered. The anisotropies are related to reorientation angles (right-hand axis) calculated under the assumption that each excited chromophore reorients by the same angle θ_i, so that the orientational average in eq 5 need not be performed. Although the relationship between anisotropy and reorientation angle is not as direct for models with inhomogeneous protein populations, the principal conclusions regarding the occurrence of chromophore reorientation are the same. The initially generated anisotropy of 0.4 in BR corresponds to an angle of 0°. A marked drop in anisotropy was observed for the L intermediate. The anisotropies of M and O determined in the present work are also plotted schematically in Figure 5. We did not attempt to determine the anisotropy of the N intermediate from our data, since the absorption profiles of N and BR overlap strongly, and complex kinetics are found in the 550−590 nm region (Váró & Lanyi, 1991). Upon formation of O the anisotropy reverts to ~0.4. An anisotropy of 0.4 is also assigned to the recovered BR population in accordance with the model developed previously to explain measurements of r_{BR} on the millisecond time scale (Wan et., 1993).

The anisotropy decay observed in Figure 2, which entails a change in the angle θ_M of ~3°, occurs on a time scale longer than the M formation time (~120 μs) but shorter than the M decay time (~3.4 ms) as measured by the TA signal. This anisotropy decay indicates a reorientation in the M state, possibly associated with a transition between two M states, M_1 and M_2. The observed decay time, 530 μs, is consistent with the decay rate from M_1 to M_2 obtained from time-resolved difference spectra (Váró & Lanyi, 1991).

The return of the anisotropy in the O state to 0.39 indicates a nearly complete recovery of the initial orientation. This result is very important for the interpretation of these results, since it shows that the anisotropy changes observed are *reversible*. They cannot be diffusive motions, associated for example with rotational diffusion of the protein inside the membrane or of membrane particles within the solution, since rotational diffusion leads to irreversible anisotropy decay. This result also confirms that rotational diffusion of small membrane particles present in the sample contributes negligibly to the present observations.

While reorientations in aqueous suspensions are more relevant physiologically, anisotropies were also measured for BR in polyacrylamide gels to permit comparison with previous studies (Czégé et al., 1982; Ahl & Cone, 1984; Der et al., 1988; Otto & Heyn, 1991). In polyacrylamide gels, evidence of reorientation is again observed in the L and M intermediates. Clearly, immobilization of the purple membrane does not eliminate all chromophore reorientations. Based on the anisotropies measured in the L and M states in gels (see Table 1), it appears, however, that the gel environment reduces the amplitude of these reorientations. The source of the restriction on this reorientation is not clear at this time. It may result from an increased viscosity in the gel environment. The anisotropy decay observed in the M state (Figure 2) is absent in the gel (Figure 3). This reorientation might involve a motion over a larger distance scale, which would be more strongly impeded by the gel environment than shorter range reorientations.

What Causes Anisotropy Changes? While the observed anisotropy changes demonstrate changes in chromophore orientation, several possible types of reorientational motions must be considered. The *trans* → *cis* isomerization itself leads to a reorientation of the retinal Schiff base transition dipole. The transition dipole is nearly parallel to the polyene chain of the retinal Schiff base (Drikos & Ruppel, 1984). Its orientation has been estimated to change by ~8° as a result of isomerization (Heyn & Otto, 1992), leading to an anisotropy drop from 0.4 to 0.39. The anisotropy in the K state (0.38 ± 0.01) may be a result of the change in dipole moment in the 13−*cis* conformation with respect to the *all-trans* conformation. Further anisotropy change could result from (1) internal motion of the chromophore within the protein pocket; (2) protein conformational changes that cause the chromophore to change orientation; or (3) rotation of BR monomers or trimers within the purple membrane. Each of these possibilities will be considered.

First, we consider chromophore motion within the protein pocket. In the BR initial state, where the pigment is held in a well-defined position in the retinal pocket (Henderson et al., 1990), the motion of the chromophore within the protein is likely to be severely restricted, and it seems unlikely that chromophore motion inside the protein on the microsecond and millisecond time scales could occur without an associated motion of the protein. Since the chromophore is tightly packed in BR, internal chromophore reorientation cannot occur without a conformational change of the protein. If the chromophore is tightly held in the intermediates as well, reorientation of the protein pocket in which the chromophore lies would be necessary for reorientation of the chromophore. Another possibility is that the chromophore is less tightly held in one or more of the photocycle intermediates. A change in protein conformation leading to more motional freedom in the protein pocket would be required for this to occur. In this case, partial randomization of chromophore reorientations within a more open protein pocket could lead to a decrease in anisotropy.

Second, anisotropy changes may track protein conformational changes, which are essential ingredients in several models of the proton-pumping mechanism in BR (Fodor et al., 1988; Henderson et al., 1990; Mathies et al., 1991). If such changes in protein conformation occur, they might cause reorientations of the chromophore detectable in anisotropy measurements.

Finally, the observed anisotropy changes may be the result of reorientational motions of the entire protein within the membrane. Any such motion, however, must be nondiffusive and reversible, as noted above. Such reorientational motion of the entire protein could not occur without exertion of a torque, triggered by photoexcitation of the chromophore. It seems difficult to conceive of such a torque arising without internal changes in the protein, such as changes in protein conformation or charge distribution. For example, the protein may rotate like a canoe paddled on one side, where the "paddle" might be motion of an α-helix against the membrane or neighboring protein.

Although the results reported here do not permit us to decide among these three possibilities, each of these sources of reorientational motion would require a change in protein conformation. Reversible internal restricted motion of the chromophore within the protein requires an opening of the chromophore pocket to a greater amplitude of chromophore motion in the K → M states, and a tightening of the chromophore pocket in the M → O stages of the photocycle. Reorientation of the protein as a whole must be driven by a torque exerted by the protein.

Role of Reorientations in Bacteriorhodopsin. The reorientations summarized in Figure 5 are associated with anisotropy changes observed in several steps in the BR photocycle: (1) in the K state; (2) in the K → L transition; (3) in the M intermediate; and (4) upon formation of the O intermediate. Reorientations also occur during the photocycle in polyacrylamide gels and were detected in the L state and with the L → M transition. The fact that reorientations are somewhat restricted by gels, where BR can nevertheless still pump protons, suggests that reorientation to the extent that occurs in suspensions is not necessary for proton pumping.

The anisotropy drop in the L and M states is consistent with previous observations that suggested differences between BR and M conformations (Bagley et al., 1982; Braiman et al., 1987; Dencher et al., 1989; Subramaniam et al., 1993). Protein conformational changes in the L and M states were proposed (Fodor et al., 1988; Henderson et al., 1990) as a mechanism to switch connectivity of the Schiff base between the proton acceptor (Asp-85) and the proton

donor (Asp-96) to facilitate deprotonation and reprotonation of the Schiff base. These steps may be associated with anisotropy decreases that are observed in the L and/or M state in gels as well as in purple membrane suspensions.

Another possible role of reorientations may be as a mechanism of information transduction to neighboring spectator proteins, which then reorient as well (Wan et al., 1993). The reorientation of neighboring proteins occurs in 1−2 ms (Wan et al., 1993) and might be induced by reorientation in the M state in photoexcited BR. The return in the O state might then induce the return of the spectator proteins, as well. Fits to a reversible reorientation model have shown that this return occurs in ~7 ms (Wan et al., 1993).

Summary. In summary, the anisotropy changes in the BR photocycle demonstrate reorientations in the K and L states, in the M intermediate associated perhaps with an $M_1 \rightarrow M_2$ step, and finally a return to the starting conformation in the O state. Although anisotropy measurements cannot distinguish between reorientations due to protein conformational changes and protein rotations, the measurements demonstrate that the reorientations are photoinduced and reversible (not diffusive) and that they are reduced somewhat but not eliminated by immobilization of the purple membrane in polyacrylamide gel. It is suggested that reorientations might correlate with changes in protein conformation that play a role in the proton-pumping mechanism or that reorientations may drive previously observed reorientations in the trimer.

ACKNOWLEDGMENT

We thank Sarah A. Mounter for assistance with preparation of bacteriorhodopsin samples. We owe thanks to Professor Roberto Bogomolni and Dr. Jorge Fukushima for sending us strain ET1-001 of *H. salinarium*, and for helpful advice on growth conditions.

REFERENCES

Ahl, P. L., & Cone, R. A. (1984) *Biophys. J. 45*, 1039−1049.
Ames, J. B., & Mathies, R. A. (1990) *Biochemistry 29*, 7181−7190.
Ansari, A., & Szabo, A. (1993) *Biophys. J. 64*, 838−851.
Bagley, K., Dollinger, G., Eisenstein, L., Singh, A. K., & Zimanyi, L. (1982) *Proc. Natl. Acad. Sci. U.S.A. 79*, 4972−4976.
Birge, R. R. (1990) *Biochim. Biophys. Acta 1016*, 293−327.
Braiman, M. S., Ahl, P. L., & Rothschild, K. J. (1987) *Proc. Natl. Acad. Sci. U.S.A. 84*, 5221−5225.
Braiman, M. S., Mogi, T., Marti, T., Stein, L. J., Khorana, H. G., & Rothschild, K. J. (1988) *Biochemistry 27*, 8516−8520.
Braiman, M. S., Bousché, O., & Rothschild, K. J. (1991) *Proc. Natl. Acad. Sci. U.S.A. 88*, 2388−2392.
Cherry, R. J., Heyn, M. P., & Oesterhelt, D. (1977) *FEBS Lett. 78*, 25−30.
Czégé, J., Dér, A., Zimányi, L., & Keszthelyi, L. (1982) *Proc. Natl. Acad. Sci. U.S.A. 79*, 7273−7277.
Dencher, N. A., Dresselhaus, D., Zaccai, G., & Büldt, G. (1989) *Proc. Natl. Acad. Sci. U.S.A. 86*, 7876−7879.
Der, A., Sander, S., & Czégé, J. (1988) *Biophys. J. 54*, 1175−1178.
Drikos, G., & Rüppel, H. (1984) *Photochem. Photobiol. 40*, 93−104.
Fodor, S. P. A., Ames, J. B., Gebhard, R., van den Berg, E. M. M., Stoeckenius, W., Lugtenburg, J., & Mathies, R. A. (1988) *Biochemistry 27*, 7097−7101.
Gerwert, K., Hess, B., Soppa, J., & Oesterhelt, D. (1989) *Proc. Natl. Acad. Sci. U.S.A. 86*, 4943−4947.
Gerwert, K., Souvignier, G., & Hess, B. (1990) *Proc. Natl. Acad. Sci. U.S.A. 87*, 9774−9778.
Godfrey, R. E. (1982) *Biophys. J. 38*, 1−6.
Gordon, R. G. (1966) *J. Chem. Phys. 45*, 1643−1648.
Grzesiek, S., & Dencher, N. A. (1986) *FEBS Lett. 208*, 337−342.
Heberle, J., & Dencher, N. A. (1990) *FEBS Lett. 277*, 277−280.
Henderson, R., Baldwin, J. M., Ceska, T. A., Zemlin, F., Beckmann, E., & Downing, K. H. (1990) *J. Mol. Biol. 213*, 899−929.
Heyn, M. P., & Otto, H. (1992) *Photochem. Photobiol. 56*, 1105−1112.
Heyn, M. P., Cherry, R. J., & Müller, U. (1977) *J. Mol. Biol. 117*, 607−620.
Holz, M., Drachev, L. A., Mogi, T., Otto, H., Kaulen, A. D., Heyn, M. D., Skulachev, V. P., & Khorana, H. G. (1989) *Proc. Natl. Acad. Sci. U.S.A. 87*, 9774−9778.
Johnson, C. K., Bostick, J. M., Mounter, S. A., Ratzlaff, K. L., & Schloemer, D. E. (1988) *Rev. Sci. Instrum. 59*, 2375−2379.
Koch, M. H. J., Dencher, N. A., Oesterhelt, D., Plöhn, H. J., Rapp, G., & Büldt, G. (1991) *EMBO J. 10*, 521−526.
Lipari, A., & Szabo, A. (1982) *J. Am. Chem. Soc. 104*, 4546−4559.
Lozier, R. H., & Niederberger, W. (1977) *Fed. Proc., Fed. Am. Soc. Exp. Biol. 36*, 1805−1809.
Mathies, R. A., Lin, S. W., Ames, J. B., & Pollard, W. T. (1991) *Annu. Rev. Biophys. Biophys. Chem. 20*, 491−518.
Nagle, J. F. (1991) *Biophys. J. 59*, 476−487.
Otto, H., & Heyn, M. P. (1991) *FEBS Lett. 293*, 111−114.
Otto, H., Marti, T., Holz, M., Mogi, T., Lindan, M., Khorana, H. G., & Heyn, M. P. (1989) *Proc. Natl. Acad. Sci. U.S.A. 86*, 9228−9232.
Schertler, G. F. X., Lozier, R., Michel, H., & Oesterhelt, D. (1991) *EMBO J. 10*, 2353−2361.
Sherman, W. V., & Caplan, S. R. (1977) *Nature 265*, 273−274.
Smith, S. O., Pardoen, J. A., Mulder, P. P. J., Curry, B., Lugtenburg, J., & Mathies, R. (1983) *Biochemistry 22*, 6141−6148.
Subramaniam, S., Marti, T., Rösselet, S. J., Rothschild, K. J., & Khorana, H. G. (1991) *Proc. Natl. Acad. Sci. U.S.A. 88*, 2583−2587.
Subramaniam, S., Gerstein, M., Oesterhelt, D., & Henderson, R. (1993) *EMBO J. 12*, 1−8.
Váró, G., & Lanyi, J. K. (1991) *Biochemistry 30*, 5008−5015.
Wan, C., Qian, J., & Johnson, C. K. (1990) *J. Phys. Chem. 94*, 8417−8423.
Wan, C., Qian, J., & Johnson, C. K. (1991) *Biochemistry 30*, 394−400.
Wan, C., Qian, J., & Johnson, C. K. (1993) *Biophys. J. 65*, 927−938.